Bioactive Materials 15 (2022) 305–315

Contents lists available at ScienceDirect

Bioactive Materials

journal homepage: www.keaipublishing.com/en/journals/bioactive-materials

Micro-ecology restoration of colonic inflammation by in-Situ oral delivery of antibody-laden hydrogel microcapsules

Bo Li [a,b], Xin Li [c], Xiaodong Chu [d], Pengcheng Lou [a,b], Yin Yuan [a,b], Aoxiang Zhuge [a,b], Xueling Zhu [a,b], Yangfan Shen [a,b], Jinghua Pan [d], Liyuan Zhang [e,f,**], Lanjuan Li [a,b,***], Zhongwen Wu [a,*]

[a] State Key Laboratory for Diagnosis and Treatment of Infectious Diseases, National Clinical Research Center for Infectious Diseases, Collaborative Innovation Center for Diagnosis and Treatment of Infectious Diseases, The First Affiliated Hospital, College of Medicine, Zhejiang University, Hangzhou, 310003, China
[b] Research Units of Infectious Disease and Microecology, Chinese Academy of Medical Sciences, Beijing, 100730, China
[c] Department of Pharmacology, The First Affiliated Hospital, College of Medicine, Zhejiang University, Hangzhou, 310003, China
[d] Department of General Surgery, The First Affiliated Hospital of Jinan University, Guangzhou, 510632, China
[e] School of Engineering and Applied Sciences, Harvard University, 9 Oxford St, Cambridge, MA, USA, 02138
[f] School of Petroleum Engineering, State Key Laboratory of Heavy Oil Processing, China University of Petroleum (East China), Qingdao, 266580, China

ARTICLE INFO

Keywords:
Antibody oral delivery
Hydrogel thin-shell microcapsules
Microfluidic
Gut microbiota
Colonic inflammation
Micro-ecology restoration

ABSTRACT

In-situ oral delivery of therapeutic antibodies, like monoclonal antibody, for chronic inflammation treatment is the most convenient approach compared with other administration routes. Moreover, the abundant links between the gut microbiota and colonic inflammation indicate that the synergistic or antagonistic effect of gut microbiota to colonic inflammation. However, the antibody activity would be significantly affected while transferring through the gastrointestinal tract due to hostile conditions. Moreover, these antibodies have short serum half-lives, thus, require to be frequently administered with high doses to be effective, leading to low patient tolerance. Here, we develop a strategy utilizing thin shell hydrogel microcapsule fabricated by microfluidic technique as the oral delivering carrier. By encapsulating antibodies in these microcapsules, antibodies survive in the hostile gastrointestinal environment and rapidly release into the small intestine through oral administration route, achieving the same therapeutic effect as the intravenous injection evaluated by a colonic inflammation disease model. Moreover, the abundance of some intestinal microorganisms as the indication of the improvement of inflammation has remarkably altered after in-situ antibody-laden microcapsules delivery, implying the restoration of micro-ecology of the intestine. These findings prove our microcapsules are exploited as an efficient oral delivery agent for antibodies with programmable function in clinical application.

1. Introduction

Colonic inflammation is a chronic inflammatory disorder resulting from immune dysregulation, which is associated with dramatic changes in the gut microbiota. To reduce the inflammation and restore the micro-ecology balance, biological treatment, such as intravenous injection of therapeutic antibodies, appears superior to other approaches [1,2], requires a large dose to achieve efficacy due to the nonspecific treatment [3]. Oral administration of therapeutic proteins and antibodies has ignited unprecedented interest attributed to its high levels of patient acceptance and long-term compliance, enhancing the therapeutic value of drugs [1,4,5]. Whereas delivering proteins and antibodies by the oral route is extremely challenging as these therapeutic proteins degrade into amino acids due to the nature of the digestive system, including extreme

Peer review under responsibility of KeAi Communications Co., Ltd.
* Corresponding author.
** Corresponding author. School of Engineering and Applied Sciences, Harvard University, 9 Oxford St, Cambridge, MA, USA 02138. ;
*** Corresponding author. State Key Laboratory for Diagnosis and Treatment of Infectious Diseases, National Clinical Research Center for Infectious Diseases, Collaborative Innovation Center for Diagnosis and Treatment of Infectious Diseases, The First Affiliated Hospital, College of Medicine, Zhejiang University, Hangzhou, 310003, China. ;
E-mail addresses: liyuanzhang@seas.harvard.edu (L. Zhang), ljli@zju.edu.cn (L. Li), wuzhongwen@zju.edu.cn (Z. Wu).

https://doi.org/10.1016/j.bioactmat.2021.12.022
Received 27 August 2021; Received in revised form 30 November 2021; Accepted 19 December 2021
Available online 25 December 2021

pH conditions, bile salt, and protease-rich environment of the gastrointestinal (GI) tract. As such, considerable efforts have been made to prevent proteolysis and denaturation of therapeutic proteins while transferring through the GI tract [6–13]; these approaches consist of chemically modifying antibodies to enhance structure stability [13], utilizing enzyme inhibitors to prevent the degradation of antibodies [12,14], and formulating delivery vehicles for antibodies [15–17]. Among these approaches, encapsulating proteins in micro- or nano-sized particles fabricated by biocompatible polymers that protect protein and peptide drugs from acid and luminal proteases in the GI tract, is the ideal strategy [18–21]. The ideal delivery particle should maintain the activity of the antibody while transferring through the stomach and rapidly release the antibodies into the small intestine. Generally, fabricating such antibody-laden particles involves mixing antibodies with polymer organic solution and rapidly extracting solvent under vigorous stirring [18,19]. During this process, therapeutic proteins are subjected to hydrodynamic shear stress originating from shaking, sonicating, and mixing [22–24], resulting in destabilizing the native conformation of protein [25–27]. A minimum amount of polymer matrix is favorable for successful particle fabrication due to the high viscosity of the therapeutic protein, and reduce the polymer consumption, leading to the low encapsulation efficiency. Releasing therapeutic proteins from antibody-laden particles in the small intestine requires rapidly enlarging pores through the degradation of the polymeric matrix, or weakening the affinity between polymeric matrix and antibody. However, polymer degradation usually can not achieve in a short period within GI tract, stimulating the pursuing of tuning the binding affinity between antibodies and polymer matrix to achieve rapid release of antibodies. The binding affinity includes electrostatic interaction, hydrogen bonding, and supramolecular interaction, which can be manipulated by adjusting pH of the microenvironment [28,29]. Due to the nature of the GI tract, there is limited space to tune the affinity through pH to achieve rapid release in the intestine. In addition, the pH in the small intestine is over the pKa of most kinds of antibody and hydrogel matrix, thus, hindering the release due to the ionic interaction between hydrogel and proteins. Therefore, an unmet need for developing a new oral delivery system to

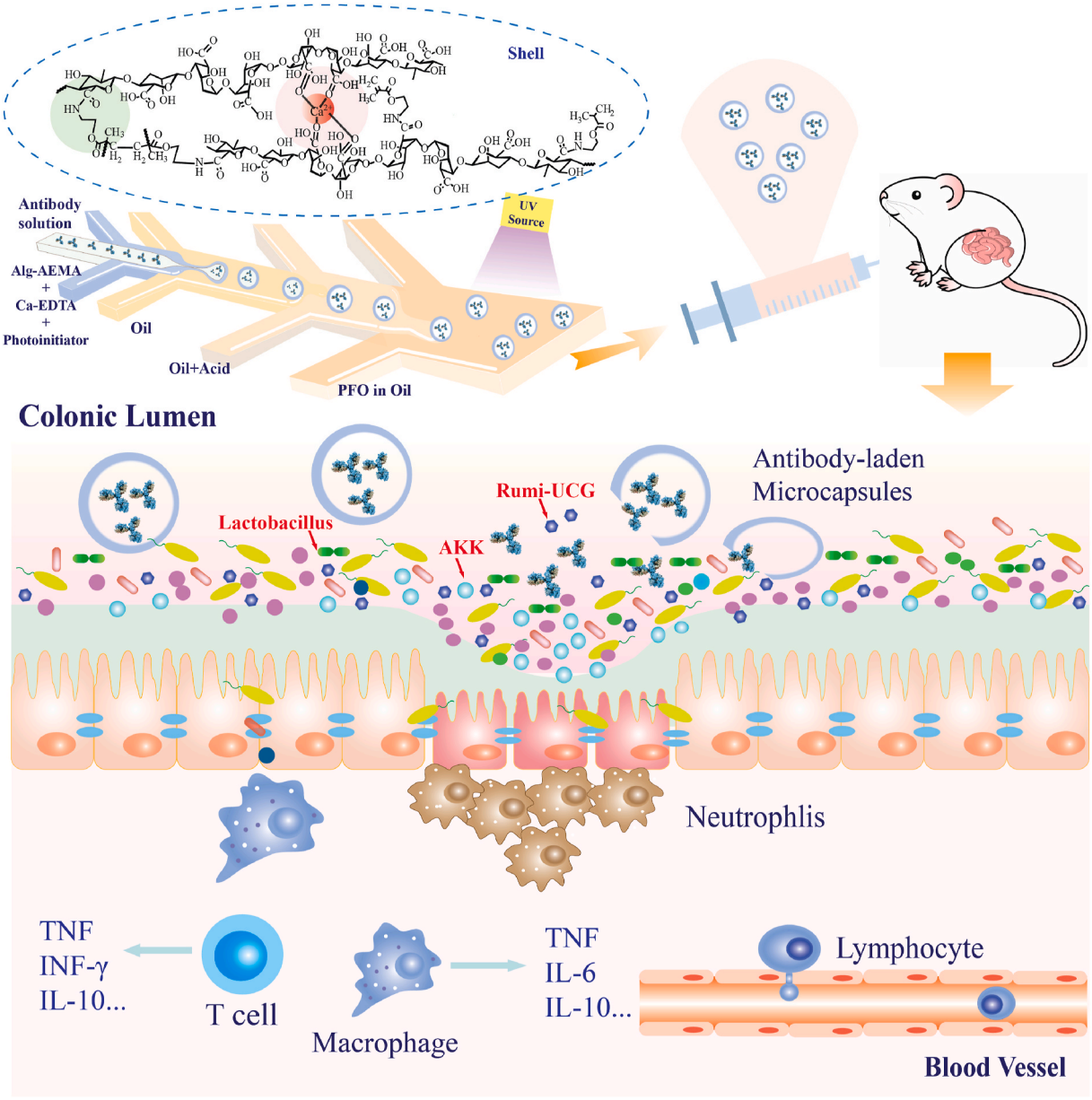

Scheme 1. Orally Administered Antibody-laden Core-shell Microcapsules for Colonic Inflammation. The core-shell microcapsules release antibodies in the colonic lumen, and reduce the inflammable reaction, thereby recreate the balance of intestinal microbiota.

protect therapeutic proteins from the stomach hostile condition and rapid release at the intestine while across the GI tract.

Here, we fabricate a thin shell hydrogel microcapsule by microfluidic technique for the oral delivery of antibodies. We first produce a water-in-water-in-oil double emulsion as the template, where water is as the inner phase and aminoethylmethylacrylate (AEMA) partially functionalized alginate as the middle phase. By sequentially Ca^{2+} ions crosslinking and C–C covalently crosslinking under UV illumination, we fabricate a thin shell microcapsule with double crosslinked network attributed to its ionic crosslinking and covalent crosslinking functionalities. The shell thickness is around 8 μm, yielding a high antibody to polymer ratio. After encapsulating antibodies in these microcapsules, we investigate the antibody release behavior at physiological neutral conditions, as well as their therapeutic effect on a mouse model with colonic inflammation, as shown in Scheme 1. We conclude that the symptom of inflammation is significantly reduced after oral delivery of antibody-laden microcapsules, achieving an advanced therapeutic effect compared with the intravenous injection at the same dose. Moreover, the micro-ecology of intestine has restored, indicated by the dramatic alteration of colonic inflammation related microorganism species in the intestine. Notably, the abundance of microbial species related to the improvement of colonic inflammation have increased after oral administration of antibody-laden microcapsules, reflecting a positive effect on colonic inflammation.

2. Result and discussion

2.1. Synthesis and characterization of crosslinkable Alg-AEMA and double network crosslinked Alg-AEMA hydrogel

To synthesize crosslinkable alginate, Alg-AEMA, we conjugate alginate with AEMA by EDC/NHS coupling chemistry, where 1-ethyl-3-(3-dimethylamino) propyl carbodiimide hydrochloride (EDC) and hydroxysuccinimide (NHS) are catalysts, as shown in Fig. 1A. The characteristic peak around 6 ppm in ^{1}H NMR spectrum of Alg-AEMA is attributed to H from the aminoethyl group on AEMA, confirming the successful synthesis of crosslinkable Alg-AEMA, as shown in Fig. 1C. The degree of methylacrylation that defines the amount of AEMA on one alginate repeat unit, plays a critical role in the mechanical property of the microcapsules shell (**Supporting Information**). Given that the modified alginate shell is supposed to retain antibodies in the core while in the stomach, small pores are beneficial, which can be obtained by controlling the amount of AEMA groups to the polymer backbone. However, the pore size of the shell can not be too small, which would inhibit antibodies releasing behavior. Thus, we vary the molar ratio of AEMA to alginate and synthesize two different types of Alg-AEMA polymers, labeling them as Alg-AEMA (5%) and Alg-AEMA (10%).

Next, we prepare Alg-AEMA bulk hydrogel with an ionic and covalent crosslinked network. First, we add 50 mM Ca-EDTA [30] into 1 wt% alginate solution with a 1:1 vol ratio, where Ca-EDTA as the crosslinker

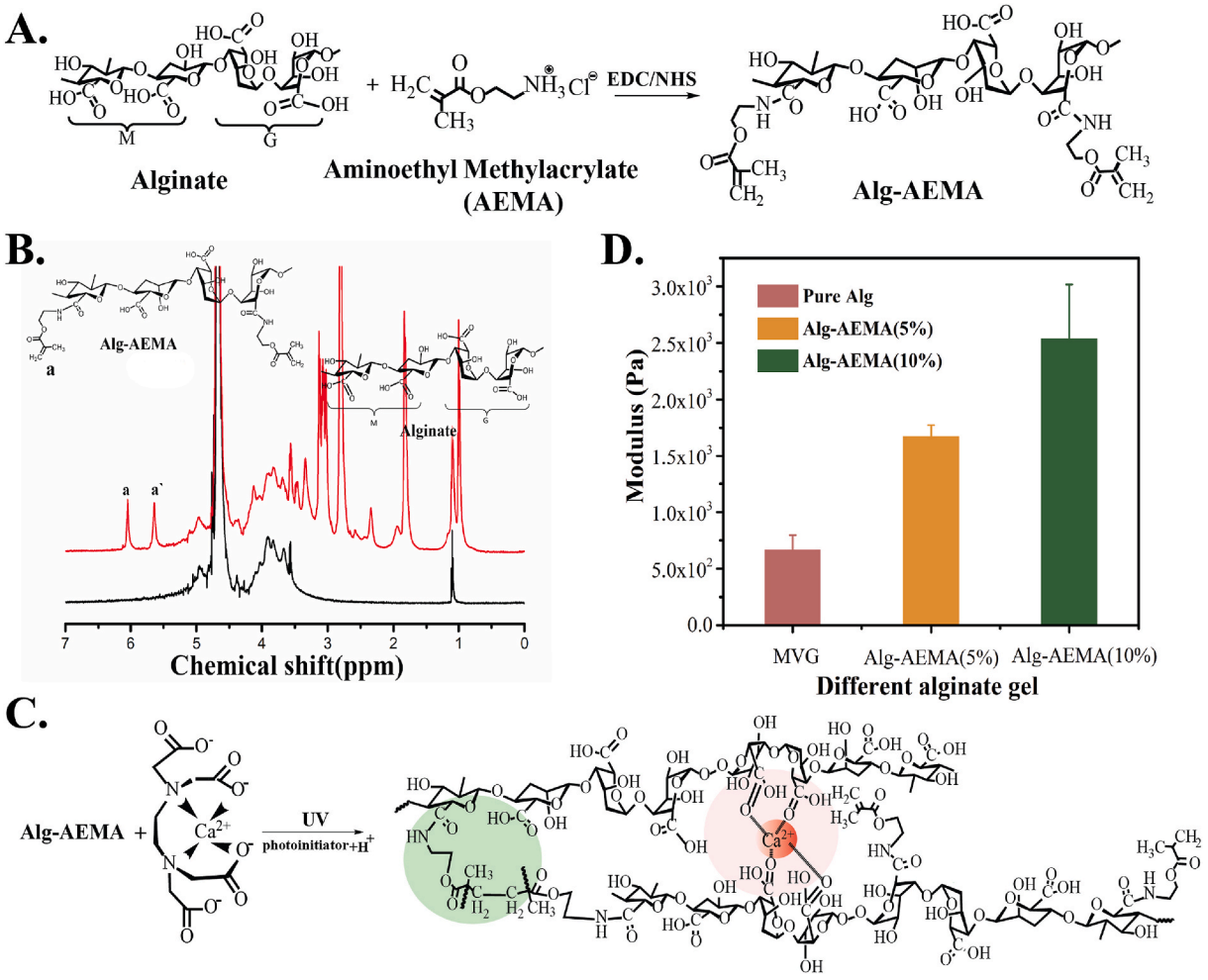

Fig. 1. Synthesis and Characterization of Alg-AEMA and Bulk Alg-AEMA. A. Reaction between aminoethylmethylacrylate and alginate by EDC/NHS coupling chemistry. **B.** Double crosslinking network of Alg-AEMA hydrogel by calcium ions crosslinking and C–C covalent bonds under UV irradiation. **C.** H NMR spectrum of Alg-AEMA and pure alginate. **D.** Mechanical property of Alg-AEMA hydrogel after double crosslinking strategy, where the green circle indicates covalent bonds and red circle indicates ionic bonds.

precursor. And then, we add 0.1% 2-hydroxy-2-methylpropiophenone solution as a photoinitiator for forming covalent bonds. By sequentially adding 0.1% acetic acid and UV illumination, we obtain the double crosslinked hydrogel by first gelling the mixture through the ionic interaction between Ca^{2+} ions and carboxylic groups, then generating covalent bonds by radical polymerization of AEMA. We prepare two kinds of bulk hydrogel by Alg-AEMA (5%) and Alg-AEMA (10%) and measure their mechanical property through AFM (Atom Force Microscope). For comparison, we prepare pure alginate bulk hydrogel with the same amount of Ca^{2+} ions as well. The elastic modulus of these two double crosslinked hydrogels increases with increasing methacrylation, as shown in Fig. 1D. The modulus of hydrogel reaches 2550 Pa when methacrylation is 10%, which is roughly 5 times higher than that of pristine alginate hydrogel. The increased modulus attributes to the

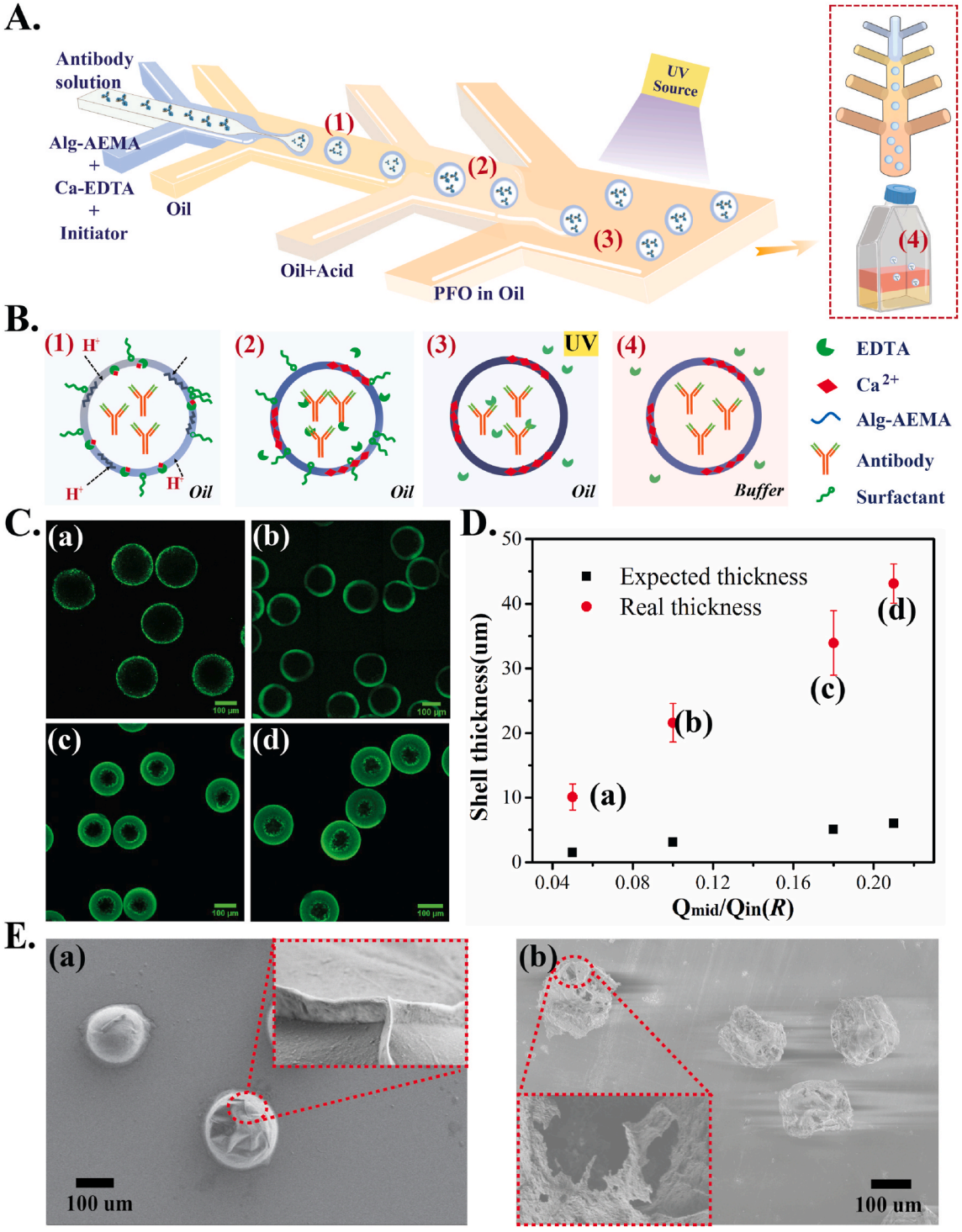

Fig. 2. Fabrication and Characterization of Thin-shell Hydrogel Microcapsules. **A**. Experiment set up for producing core-shell hydrogel microcapsules. **B**. The mechanism of generation of core-shell microcapsules. **C**. Confocal microscope image of core-shell microcapsules with different shell thickness, where the alginate shell is labeled with fluorescein isothiocyanate (FITC). **D**. Shell thickness as a function of flow rate ratio ***R***, defined by the middle alginate phase to inner aqueous phase. **E**. SEM images of thin-shell hydrogel Alg-AEMA (10%) microcapsules(a), and pure alginate microcapsules(b). The inserted image is the magnified image of microcapsules surface.

covalent C–C double bonds after UV irradiation, which significantly decreases the mesh size of hydrogel, ξ_{mesh}, according to classical rubber elasticity theory. The mesh size of two hydrogels is 13 nm and 10 nm for Alg-AEMA (5%) and Alg-AEMA (10%), respectively, calculated by $\xi_{mesh} = [k_BT/G]^{1/3}$, where k_B is Boseman constant, T is the temperature in Fahrenheit, and G is the modulus [31,32]. The pore sizes of these two hydrogels are both large enough for antibodies to transport. Considering the mechanical property of the capsule shell is critical for enduring the hostile condition while across the GI tract, we arbitrarily choose Alg-AEMA (10%) for the following experiment, where we label its name as Alg-AEMA.

2.2. Fabrication and characterization core-shell hydrogel microcapsules

To prepare a core-shell alginate microcapsule, we first generate water-in-water-in-oil double emulsion as the template by a co-flow microfluidic device, as shown in Fig. 2A. The inner phase is the aqueous phase, and the middle phase is Alg-AEMA with a concentration of 1 wt%. We add 0.1% of photoinitiator in the Alg-AEMA phase for photo-crosslinking and 50 mM Ca-EDTA as an ionic crosslinker. These two aqueous phases are emulsified in fluorinated oil (3 M™ Novec™ 7500) phase, containing 1% Krytox as the surfactant, and form a temporary double emulsion, corresponding to Fig. 2B(1). These emulsions will be transited into another oil phase with the same components as the first oil phase but containing extra 0.1% acetic acid. The rapid diffusion of acid into the alginate shell phase enables releasing Ca^{2+} ions from Ca-EDTA and forms the alginate hydrogel shell, corresponding to Fig. 2B (2). Afterward, we inject these emulsions into the third oil phase with perfluorinatedoctanol (PFO), as shown in Fig. 2B(3). The PFO destabilizes the oil/water interface by possibly replacing surfactant or destroy the rigid pattern of the surfactant at the interface [33], which allows the direct transition into the aqueous phase without extra rinsing steps, as shown in Fig. 2B(4). This direct transition of microcapsules from the oil phase into the aqueous phase minimizes the time scale for antibody immersing in the acidic solution.

The shell thickness has a great impact on the mechanical property, which is predominantly determined by the flow rate ratio, R, between the middle phase and inner aqueous phase. Due to the low refractive index of hydrogel, it is difficult to directly measure the shell thickness of alginate microcapsules in the aqueous solution. Thus, we chemically modify Alg-AEMA with fluorescein isothiocyanate (FITC), allowing us to observe and measure the shell thickness under a microscope. When $R = 0.05$, the shell thickness is 10 μm, measured by the confocal microscope, as shown in Fig. 2C(a). This value is larger than the expected value from the flow rate ratio(R), 1.5 μm, denoted by black squares in Fig. 2D. When $R = 0.1$, the shell thickness increases to 21.6 μm, which is larger than the expected value of 3.1 μm as well, as shown in Fig. 2C(b). While increasing R to 0.18 and 0.2, the shell thickness is 34 μm and 43 μm, respectively, where the expected value is 5.1 μm and 6 μm, as shown in Fig. 2C(c) and Fig. 2C(d). The significant difference between the actual value and the expected value should be attributed to the diffusion and the convection of Alg-AEMA molecules induced by the shear stress from the channel during the transition into the acid oil phase. Based on Fick's law, the diffusion distance of Alg-AEMA is the same for different flow rate ratios. Thus, the increased value for shell thickness largely depends on the convection induced by fluid movement. Moreover, the difference between the actual and the expected value of shell thickness increases when R increases; this dictates the convection dominants the molecular motion before crosslinking.

To observe the morphology of the double network crosslinked microcapsules, we lyophilize the microcapsules at −80 °C to preserve their integrity and characterize the morphology by scanning electron microscopy (SEM). Alg-AEMA microcapsules maintain their integrity after the freeze-drying process, exhibiting a smooth surface, as shown in Fig. 2E (a). By contrast, the microcapsules fabricated by original alginate are raptured during the freeze-drying process, illustrated in the inserted image of Fig. 2E(b). The cracks on the shell should be account for the ice crystal that immediately formed inside the core during the freeze-drying process and punctures the shell. On the contrary, the integrated shell of the Alg-AEMA microcapsules proves that the mechanical property has significantly enhanced after double crosslinking; this double crosslinked network is favorable for these microcapsules to sustain the harsh condition during oral administration. This integrated shell also corresponds to the mechanical property characterization, where the modulus of Alg-AEMA is much larger than that of original alginate hydrogel, as shown in **Fig. 1D.**

2.3. Release kinetics of monoclonal antibody ex vivo

To evaluate the encapsulation ability of microcapsules, we prepare antibody-laden microcapsules with the same approach by replacing the inner phase with a model fluorescent antibody solution (Molecular weight~160 KD, Alexa Fluor® 488 Goat Antibody). We maintain the flow rate ratio at a minimum value to reach a high loading antibody efficiency, obtaining microcapsules with the shell thickness around 10 μm. The fluorescent antibodies are successfully loaded in the microcapsules, verified by the homogeneously distributed fluorescent signals, as shown in **Fig. 3A(a–d)**. These microcapsules own an excellent ability for retaining antibodies, confirmed by the long-term retention of strong fluorescent signals over one month (Fig. 3A(d)). This slow-release behavior should be attributed to the double crosslinked network of the shell, as there are limited factors can affect the pore size of the shell while in water. We further quantify the antibody retention ratio as a function of time by measuring the fluorescent intensity at the focal plane of microcapsules. We find around 25% of antibodies remain inside the microcapsules after one month, which indicates the excellent encapsulation ability of the modified microcapsules, as shown in Fig. 3A(e).

To elucidate the effect of microcapsules on the released antibody, circular dichroism (CD) analysis is performed. We encapsulate Infliximab into Alg-AEMA microcapsules, an anti-Tumor Necrosis Factor-α (*anti*-TNF-α) monoclonal antibody that blocks TNF-α from binding to the intestinal cell surface receptor for colonic inflammation treatment. After releasing from microcapsules at physiological condition, the solution is dialyzed at room temperature prior to CD measurement [34–36]. The far-UV wavelength spectra of released Infliximab, shows no difference in the shape or degree of ellipticity compared to pristine Infliximab. Moreover, the CD spectra show a minimum at 218 nm, which is a typical manifestation for β-sheets, the predominant secondary structure of monoclonal antibody [37,38], as shown in Fig. 3B. This result confirms the structural conformation of Infliximab is retained after releasing from microcapsules, implying the releasing process from microcapsules does not damage the secondary structure of antibodies.

To investigate the release profile of the antibody at the physiological condition during oral administration, we first characterize their release profile under a weak acid condition, mimicking antibody transferring through the stomach. The buffer that we choose with pH is around 5, as we flush the stomach with buffer to further eliminate the acid influence the during the animal experiment. Surprisingly, there are more than 85% antibodies remaining inside these microcapsules for the first 2 h, exhibiting an excellent capability of retaining antibodies under acidic conditions, as shown in Fig. 3C(a). This high retain ratio of antibodies in microcapsules should primarily be attributed to the secondary amine groups from AMEA that block the H^+ ions in the acidic solution [39]. Moreover, the protonated amines further interact with carboxylic groups through electrostatic interaction, which further compacts the shell and delays the antibody release. Compared with the antibodies that being encapsulated in the microcapsules prepared by pristine alginate, the release period is as quickly as 5 min (**Supporting Information**, Fig. S1). These results indicate that the double crosslinked hydrogel shell can maintain the antibodies inside for a longer time. In addition, these extra amine groups in the shell enable the easy adhesion to the mucus layer, while is favorable for prolonging the duration time in the intestine

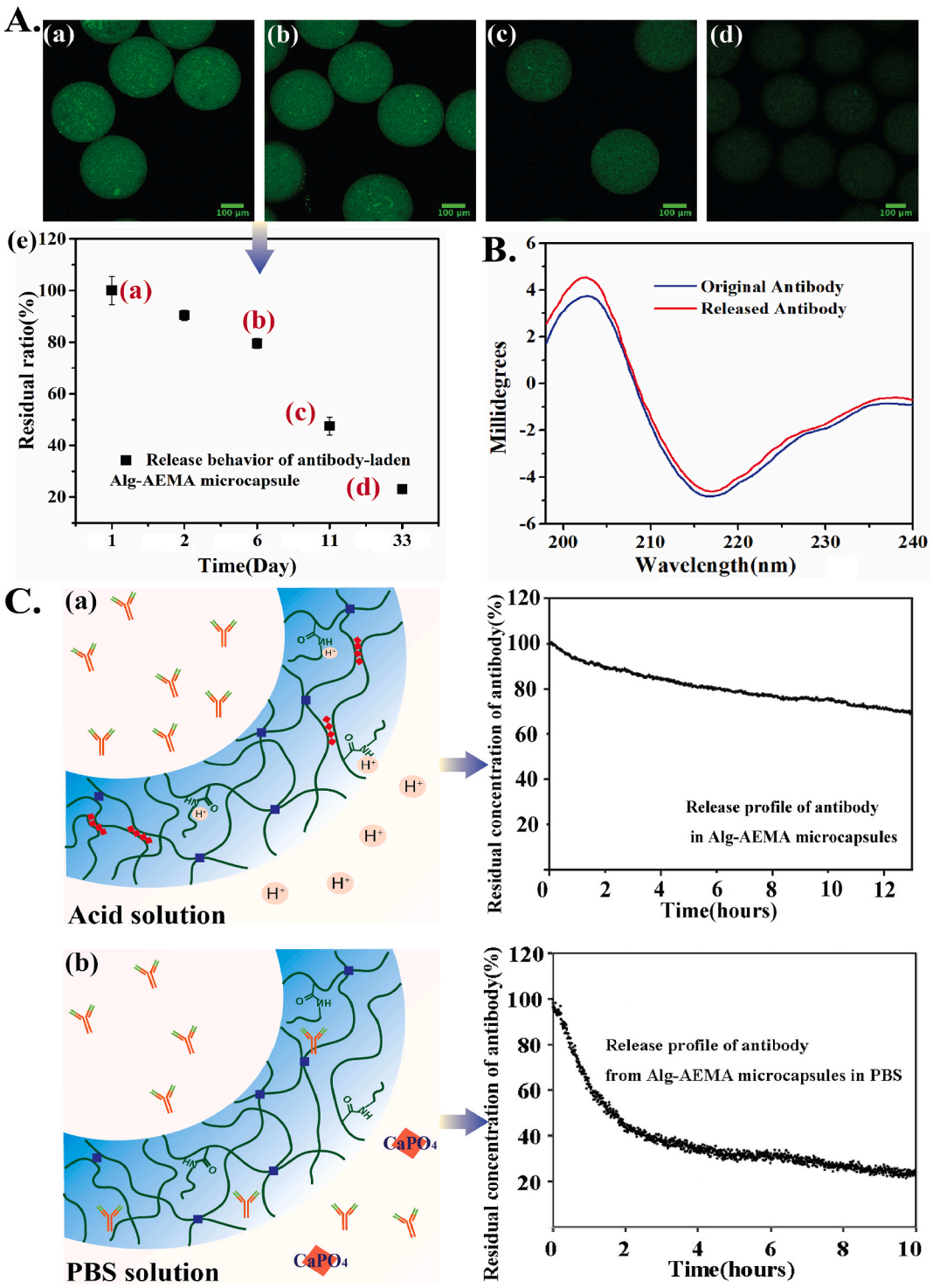

Fig. 3. Release of Antibody-laden Core-shell Microcapsules without Compromised Function *in vitro*. **A.** Releasing fluorescent model antibody from microcapsules at different time point. **B.** Circular dichroism for original antibody and antibody released from microcapsules under physiological condition. **C.** Releasing profile under acid solution(b), and in PBS solution(c) with different mechanism.

during oral delivery.

To check the release behavior at neutral condition, we immerse these microcapsules in the PBS buffer to mimic the intestinal microenvironment and characterize the fluorescent intensity at different time scale. The antibody shows a rapid release behavior in the first 2 h and gradually slows down the releasing rate. After 10 h, there are only 20% antibodies left in microcapsules, as shown in Fig. 3C(b). The fast release behavior in the first 2 h is mainly attributed to the enlarged pores of the hydrogel shell, arising from the dissociation of Ca-Alginate in the presence of PBS. This release profile of antibodies proves that the microcapsules respond to different conditions by different mechanisms enabling programmable deliver of antibodies in the physiological condition.

2.4. Oral administration of monoclonal antibody-laden microcapsules

To investigate the pre-clinical capability of microcapsules in oral delivery of antibodies, we first create an inflammatory bowel disease mouse model by orally taking dextran sodium sulfate (DSS, Fig. 4A, **Supporting Information**); this induces epithelial damage with anticoagulant properties of mice, resulting in compromised mucosal barrier function [40,41]. We then divide these mice into six groups (n = 6) and treat each group with saline, bare microcapsules, antibody-laden microcapsules, orally administrating, and intravenous injecting antibody (Infliximab). We label them as Control group, DSS group, BM group, AM group, OA group, and IV group, respectively. The weight of the mice in AM group gradually increases after oral administration of antibody-laden microcapsules, presenting similar trending compared with IV group, as shown in Fig. 4A(a). Although the difference of spleen weight between each group is negligible as shown in **Fig. 4A(b)**, the length of the colon for antibody-laden microcapsules treated mice is similar to that of the healthy group, as shown in Fig. 4A(c). Moreover, we characterize the symptom of the mice in a quantitative way by DAI (disease activity index) that evaluating the condition of mice based on weight loss, stool shape, and fecal occult blood, where 0 defines the normal health condition and 4 defines the worst physiological condition, such as fecal blood (**Supporting Information**, Table S1). **Among treatment disease groups, the DAI score for AM group is the lowest,**

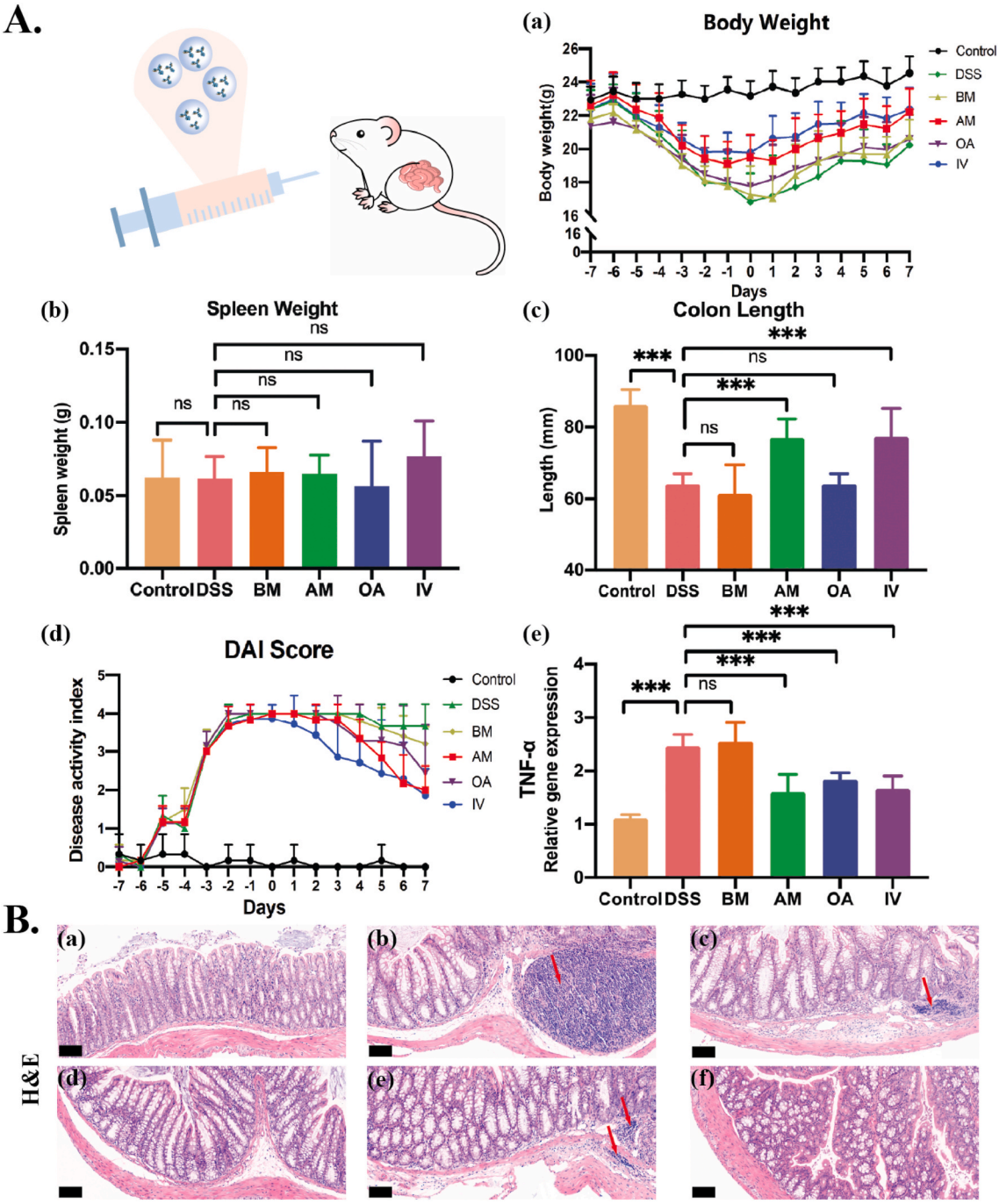

Fig. 4. Antibody-laden Microcapsules Alleviate Colonic Inflammation. A. Body weight loss (a), spleen length (b), colon length (c), DAI score (d), and TNF-α (e). **B.** H&E staining of control group(a), DSS group(b), BM group(c), AM group(d), OA group(e) and IV group(f), respectively. Red arrows show the neutrophils and lymphocytes infiltrating into the mucosal and submucosal layer.

decreasing to 2 with no fecal occult blood, which is roughly the same as IV group (Fig. 4A(d)). In contrast, the DAI of OA group is about 3 with the sign of occult blood in the feces. These results suggest that the antibody-laden microcapsules alleviate the IBD symptoms, similar to that of the traditional intravenous injection.

Previously report has proved that the disordered intestinal microbiota is one of the main reasons causing colonic inflammation. After the destruction of the intestinal epithelial mucosal barrier, the abnormal immune response from colonic inflammation is exacerbated by the secreted inflammatory factors like TNF-α at the inflammatory area. In turn, epithelium cells exposed to intestinal microbiota further promote the immune cell response. By binding with TNF-α, the released Infliximab blocks the affinity between TNF-α and cell surface receptors and maintains the intestinal microecological balance. To verifying its efficacy, we perform the qPCR test, where shows the expression level of TNF-α of AM group is the lowest compared with other treatment groups, as shown in Fig. 4A(e). Moreover, the intestinal section of mice from AM group exhibits an intact inner structure with no inflammatory cell infiltration and hyperemic edema, proved by H&E staining (hematoxylin and eosin staining), as shown in Fig. 4B. In contrast, other samples present a thickening intestinal wall with a disordered villi structure. We also observe that the infiltration of neutrophils and lymphocytes into the mucosal and submucosal layer, especially for OA group. These results validate that functionalized alginate-microcapsules shield antibodies from hash conditions, still maintain their activity after in-situ releasing at the small intestine.

2.5. *Core-shell microcapsules reinforce the efficacy of infliximab*

Myeloperoxidase (MPO), the most abundant neutrophil granule protein, is of prime importance in microbicide activity. After being released extracellularly at inflammatory sites, it is easy to induce inflammation or damage of the host tissue. The significantly decreased MPO expression level is presented by the reduced number of brown cells in MPO staining section. Mice in AM group declare reduced MPO positive cells similar to that of IV group and control group, as shown in Fig. 5A(a-f). By contrast, a mass of MPO-positive cells still exist in OA group, as shown in Fig. 5A(e). Compared with directly orally taking antibodies, encapsulation changes the antibody administration route while shielding the damage from the digestive tract during oral administration. After neutralizing the overexpressed TNF-α, encapsulated antibodies efficiently block TNF-α from binding to the intestinal cell surface receptors, enhance the intestinal inflammatory response, and protect the intestinal barrier. Thus, it helps to recover the inflammatory intestine and exert an antagonistic effect against harmful bacteria.

Tight junction protein (ZO-1) is a critical component of the physical and biological barrier of the intestinal mucosa. It forms a family of tight junction proteins in the intestinal epithelial barrier to close gaps between epithelial barrier cells [42]. During the development of inflammatory bowel disease, the mucosal barrier of intestinal epithelial cells is destroyed, inducing a disordered intestinal microorganism balance. The destruction of the intestinal mucosal layer further leads to an increase in intestinal permeability, causing the adhesion of pathogens and the recurrence of inflammation for DSS group [43]. The restoration of the intestinal mucosal layer is critical for maintaining the epithelial cell polarity and material delivery efficacy as well as blocking the occurrence and development of intestinal wall inflammation. After orally administrating antibody-laden microcapsules, ZO-1 immunostaining staining presents continuously green lines along the edge of the epithelial cells, which reflects the restoration of the intestinal mucosal layer, as shown in Fig. 5B. Moreover, the microvilli pattern in AM group is well structured compared to the IV group and the control group. By contrast, the villi structure is destroyed for mice in DSS group with a sparse and irregular pattern, confirmed by the discrete green line. We observe similar damaged structure for the tight junction of the top of villi, as well as the intestinal crypt in OA groups, implying the compromised intestinal barrier function [44]. Furthermore,

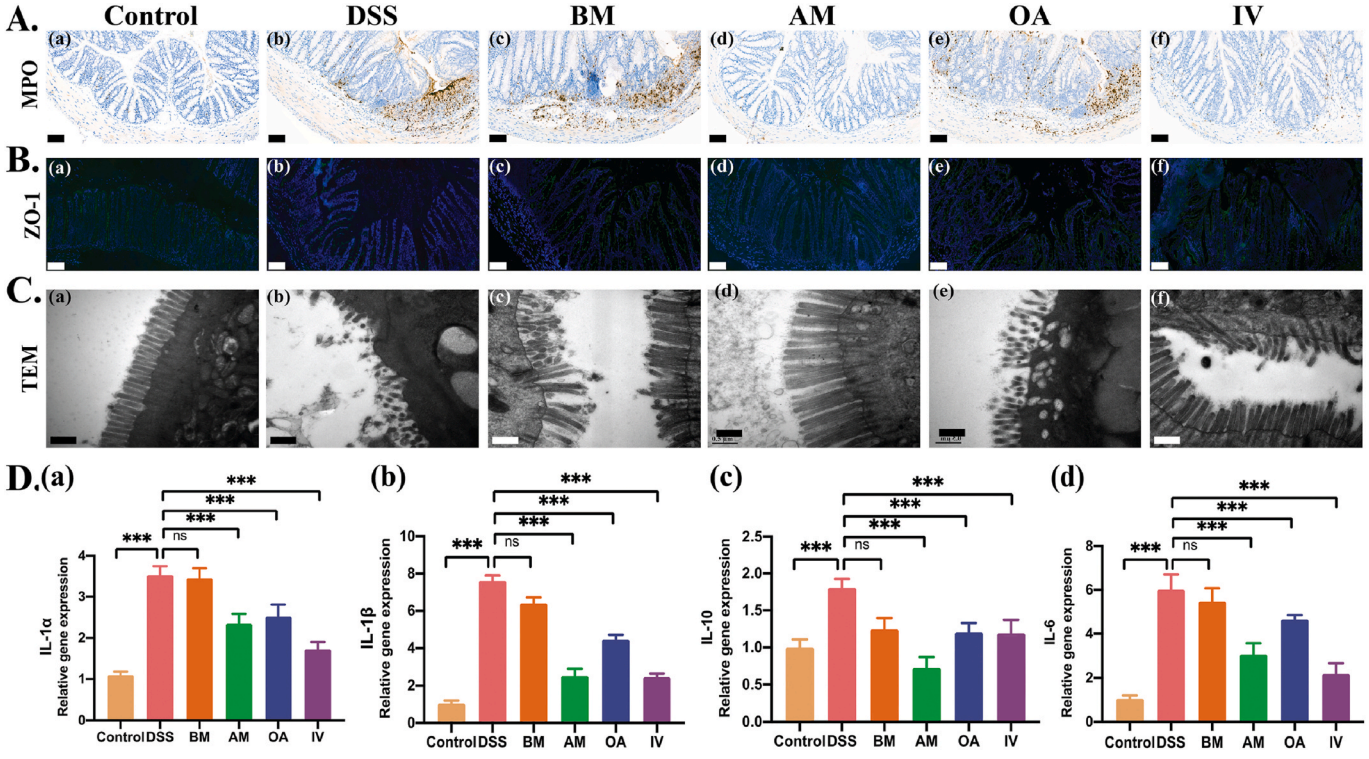

Fig. 5. Antibody-laden Microcapsules Ameliorate Gut Barrier Function. MPO (**A**) and ZO-1 (**B**) and TEM (**C**) for control group and disease model groups. (a) is control group, (b) is DSS group, (c) is BM group, (d) is AM group, (e) is OA group, and (f) is IV group. **D**. The concentration of cytokine, IL-10, IL-6, IL-1β, and IL-1α, for each group ($n = 6$, $p < 0.05$).

transmission electron microscope (TEM) images confirm the intact intestinal epithelial cell structure, including more completely aligned and patterned microvilli for AM group, where microvilli of the intestinal epithelial cells in OA is ruptured, sparse, and stunted along with the breakdown of the brush border, as shown in Fig. 5C. These results show that the intestinal epithelial barrier function of the antibody-laden microcapsules group is completely repaired by antibody-laden microcapsules, which is favorable for healing and improving the micro-environment of the intestine.

We further quantify the inflammation-associated cytokine expression level after seven days by quantitative PCR. After orally taking antibody-laden microcapsules, the expression level of cytokines, IL-1α, IL-1β, IL-6, and IL-10, of AM group has significantly decreased ($n = 6$, $p < 0.05$) compared with disease model groups. Of all groups for investigating the capability of secreting cytokines, AM group shows the lowest expression level for most cases, matching the expression level of intravenous injection administration, as shown in Fig. 5D. This result validates the antibody is capable of binding with TNF-α after releasing from microcapsules through an oral administration for efficient colonic inflammation treatment.

2.6. Antibody-laden microcapsules alleviate microbial dysbiosis

To investigate the variation of intestinal microbiota for each group under different treatment strategies, we sequence the 16 SrRNA at V3–V4 region of the microbiota and category OTU cluster with a

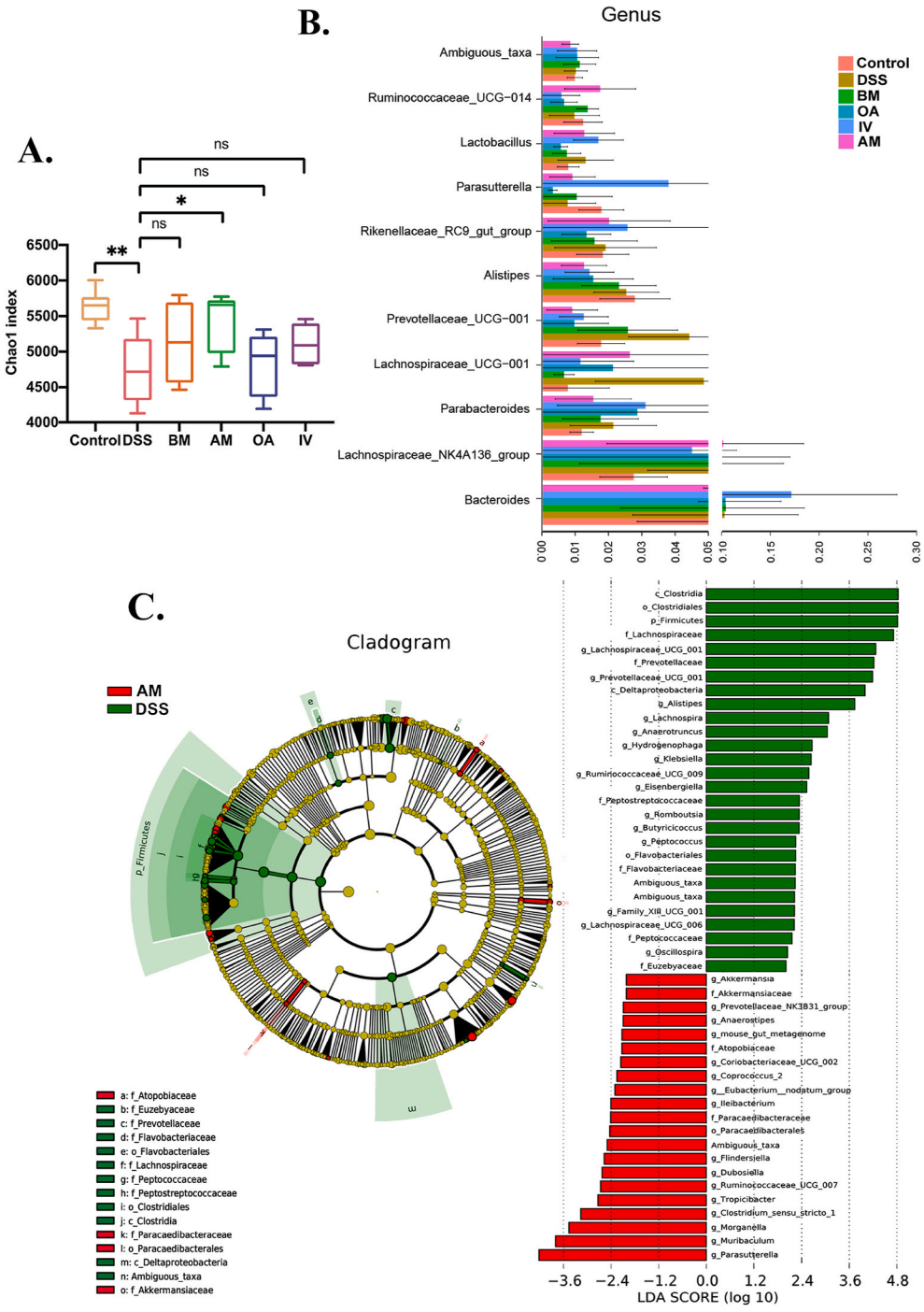

Fig. 6. Antibody-laden Microcapsules Restore Micro-ecology Balance of Gastro Intestine. A. The α-diversity of gut microbiota determined by Chao1 index among control groups and treatment group. Relative abundance of taxa at different genus (**B**) and family level (**C**). At family level, green indicates a high-level taxon in the DSS group, and red indicates a high-level taxon in the AM group. Rings from inside out represents phylum to genus level, and sizes of circles indicate relative abundance of the taxon.

similarity of 97% based on RDP classifier Bayesian algorithm. Thus, the index of OTU number calculated by Chao1 algorithm is applied to evaluate the species abundance and diversity of the intestinal microbiota. The intestinal microbiota is upregulated in their community abundance for AM group compared with control group, as shown in Fig. 6A. As the disruption of intestinal microbiota is one of the main reasons for colonic inflammation, we evaluate the community abundance of intestine microbiota at the genus and family levels to further investigate the variation of intestine microbiome after Infliximab treatment. In the development of IBD, the diversity and community abundance of intestinal microbiota are generally declined, accompanied by the variation of some specific species, especially for the diversity and the community abundance of Clostridium spp. and Faeculaceae [41]. Previously studies reveal that the community abundance of Clostridiales and Lachnospiraceae that relate to the improvement of intestinal inflammation symptoms has increased after antibody treatment, which is confirmed by the increase of Lachnospiraceae in AM groups [40,45]. Moreover, a significant increase in the intestinal microbiota abundance of Bacteroides, Lactobacillus and Parasutterella at the family level for IV group, which may be related to the improvement of intestinal inflammation as well. We also observe a similar upregulation trend in the relative percentage for Lachnospiraceae_UCG-001 and Lachnospiraceae_NK4A136 at the genus level for AM group, implying the positive effect of antibody-laden microcapsules on intestinal inflammation (Fig. 6B). In addition, other species that are favorable for the maintenance of the intestinal microecological balance, such as AKK, Paraceaedibateraceae, and Rumi-UCG-007, exhibit similar enriched abundance behavior analyzed from taxonomic abundance (Fig. 6C). Subsequently, we statistically analyze the species in community abundance for AM group, IV group, and DSS group [46]. Overall, the intestinal microbiome structure of IV group and AM group is reconstructed compared with DSS group (Fig. S2), appearing more intestinal probiotics. These results indicate that the antibodies effectively bind to TNF-α after releasing from microcapsules and regulate the mouse intestinal microorganisms to re-establish and restore the balance of intestinal microenvironment by oral administration [47]. These results are consistent with the previous study that Infliximab directly acts on the site of inflammation, promoting the growth of the mucus layer and helping to regulate the effect of intestinal microbiota on IBD [45].

3. Conclusion

A new microfluidic-based thin-shell hydrogel microcapsule for oral delivering antibodies is fabricated to address the challenge of antibody activity loss while orally transferring through the gastrointestinal tract. By generating the double crosslinking network of the shell and manipulating the flow ratio of the shell phase, we obtain thin shell microcapsules with strong mechanical properties as an oral delivery agent. After releasing from the microcapsules, antibodies preserve their conformation and effectively bind to TNF-α that enhances immunogenetic reaction, achieving the same therapeutic effect compared with the traditional intravenous injection therapy; this also confirms the effectiveness of microcapsules in antibody protection. We study the community abundance of intestinal microbiota after antibody-laden microcapsules treatment, where the richness of intestinal microorganisms being attributed to the improvement of colonic inflammation has dramatically increased, such as Clostridiales, Enterobacteriaceas, and Lachnospiraceae. Although the richness of gut microbiota has significantly altered which is similar to the intravenous injection treatment, larger-scale clinical data is required to distinguish the critical role of antibody-laden microcapsules in favor of certain probiotic species. Overall, our microcapsules may provide a general framework for studying the mechanism of TNF-α antagonists blocking TNF-α, affecting the intestinal microecological balance and IBD development.

Declaration of interests

☒ The authors declare that they have no known competing financial interests or personal relationships that could have appeared to influence the work reported in this paper.

☐The authors declare the following financial interests/personal relationships which may be considered as potential competing interests:

Data and materials availability

All data are available in the main text or the supplementary materials.

CRediT authorship contribution statement

Bo Li: generate, Methodology, carried out all experiment, Formal analysis, reviewed and approved the manuscript. **Xin Li:** carried out all experiment, Formal analysis, reviewed and approved the manuscript. **Xiaodong Chu:** carried out all experiment, Formal analysis, reviewed and approved the manuscript. **Pengcheng Lou:** carried out all experiment, Formal analysis, reviewed and approved the manuscript. **Yin Yuan:** reviewed and approved the manuscript. **Aoxiang Zhuge:** carried out all experiment, analysis. **Xueling Zhu:** carried out all experiment, analysis. **Yangfan Shen:** reviewed and approved the manuscript. **Jinghua Pan:** help to analysis the bioinformatic analysis, reviewed and approved the manuscript. **Liyuan Zhang:** generate, Methodology, reviewed and approved the manuscript. **Lanjuan Li:** generate, Methodology, reviewed and approved the manuscript. **Zhongwen Wu:** generate, Methodology, reviewed and approved the manuscript.

Declaration of competing interest

All other authors declare they have no competing interests.

Acknowledgments

We acknowledge research funding support from the National Key Science and Technology Project of China (grant number 2018YFC2000500, 03), National Natural Science Foundation of China 81703430 and 81803449, CAMS Innovation Fund for Medical Sciences (grant number 2019-I2M-5-045) and the Natural Science Foundation of Zhejiang Province (LYY20H300003). Especially, thanks to KW Liu, The youth of self-confidence and spiritual support. The authors especially thank to H&L Biotherapeutic Inc for the Microfluidic Biocompatible Encapsulation Platform.

Appendix A. Supplementary data

Supplementary data to this article can be found online at https://doi.org/10.1016/j.bioactmat.2021.12.022.

References

[1] A.C. Anselmo, Y. Gokarn, S. Mitragotri, Nat. Rev. Drug Discov. 18 (2019) 19.
[2] H.C. Zierden, A. Josyula, R.L. Shapiro, H.T. Hsueh, J. Hanes, L.M. Ensign, Trends in Molecular Medicine, 2021.
[3] N. Zmora, D. Zeevi, T. Korem, E. Segal, E. Elinav, Cell Host Microbe 19 (2016) 12.
[4] M. Durán-Lobato, Z. Niu, M.J. Alonso, Adv. Mater. 32 (2020) 1901935.
[5] S. Mitragotri, P.A. Burke, R. Langer, Nat. Rev. Drug Discov. 13 (2014) 655.
[6] J. Li, D.J. Mooney, Nat. Rev. Mater. 1 (2016) 1.
[7] X. Qin, C. Yu, J. Wei, L. Li, C. Zhang, Q. Wu, J. Liu, S.Q. Yao, W. Huang, Adv. Mater. 31 (2019) 1902791.
[8] A.C. Daly, L. Riley, T. Segura, J.A. Burdick, Nat. Rev. Mater. 5 (2020) 20.
[9] J. Wang, B. Li, M.X. Wu, Proc. Natl. Acad. Sci. Unit. States Am. 112 (2015) 5005.
[10] A. Abramson, E. Caffarel-Salvador, M. Khang, D. Dellal, D. Silverstein, Y. Gao, M. R. Frederiksen, A. Vegge, F. Hubálek, J. J. Water, *Science*. 363 (2019) 611.
[11] B.B. Hsu, I.N. Plant, L. Lyon, F.M. Anastassacos, J.C. Way, P.A. Silver, Nat. Commun. 11 (2020) 1.
[12] N.G. Lamson, A. Berger, K.C. Fein, K.A. Whitehead, Nature biomedical engineering 4 (2020) 84.

[13] C.K. Wang, D.J. Craik, Nat. Chem. Biol. 14 (2018) 417.
[14] C. Zhong, P. Li, S. Argade, L. Liu, W. Liang, H. Xin, B. Eliceiri, B. Choudhury, N. Ferrara, Nat. Commun. 11 (2020) 1.
[15] Y. Lee, K. Sugihara, M.G. Gillilland, S. Jon, N. Kamada, J.J. Moon, Nat. Mater. 19 (2020) 118.
[16] N. Veiga, M. Goldsmith, Y. Granot, D. Rosenblum, N. Dammes, R. Kedmi, S. Ramishetti, D. Peer, Nat. Commun. 9 (2018) 1.
[17] Z. Cao, X. Wang, Y. Pang, S. Cheng, J. Liu, Nat. Commun. 10 (2019) 1.
[18] R.D. Vaishya, A. Mandal, M. Gokulgandhi, S. Patel, A.K. Mitra, Int. J. Pharm. 489 (2015) 237.
[19] A. Vila, A. Sanchez, M. Tobıo, P. Calvo, M. Alonso, J. Contr. Release 78 (2002) 15.
[20] P. He, H. Liu, Z. Tang, M. Deng, Y. Yang, X. Pang, X. Chen, Int. J. Pharm. 455 (2013) 259.
[21] C. Damgé, M. Socha, N. Ubrich, P. Maincent, J. Pharmaceut. Sci. 99 (2010) 879.
[22] W. Wang, Int. J. Pharm. 185 (1999) 129.
[23] W. Wang, Int. J. Pharm. 289 (2005) 1.
[24] M.-H. Morel, A. Redl, S. Guilbert, Biomacromolecules 3 (2002) 488.
[25] Z. Bryant, V.S. Pande, D.S. Rokhsar, Biophys. J. 78 (2000) 584.
[26] P.-C. Li, D.E. Makarov, J. Chem. Phys. 119 (2003) 9260.
[27] I.B. Bekard, P. Asimakis, J. Bertolini, D.E. Dunstan, Biopolymers 95 (2011) 733.
[28] N.A. Peppas, A.R. Khare, Adv. Drug Deliv. Rev. 11 (1993) 1.
[29] E.R. Edelmana, A. Nathan, M. Katada, J. Gates, M.J. Karnovsky, Biomaterials 21 (2000) 2279.
[30] L. Zhang, K. Chen, H. Zhang, B. Pang, C.H. Choi, A.S. Mao, H. Liao, S. Utech, D. J. Mooney, H. Wang, Small 14 (2018) 1702955.
[31] P.J. Flory, J. Rehner Jr., J. Chem. Phys. 11 (1943) 512.
[32] A. Kuijpers, G. Engbers, J. Feijen, S. De Smedt, T. Meyvis, J. Demeester, J. Krijgsveld, S. Zaat, J. Dankert, Macromolecules 32 (1999) 3325.
[33] A.B. Theberge, E. Mayot, A. El Harrak, F. Kleinschmidt, W.T. Huck, A.D. Griffiths, Lab Chip 12 (2012) 1320.
[34] S. Wirtz, M.F. Neurath, Adv. Drug Deliv. Rev. 59 (2007) 1073.
[35] Y.L. Jones-Hall, M.B. Grisham, Pathophysiology 21 (2014) 267.
[36] J.R. Maxwell, J.L. Viney, Current Protocols in Pharmacology 47 (2009), 5.57. 1.
[37] K. Chen, D.S. Long, S.C. Lute, M.J. Levy, K.A. Brorson, D.A. Keire, J. Pharmaceut. Biomed. Anal. 128 (2016) 398.
[38] V. Joshi, T. Shivach, N. Yadav, A.S. Rathore, Anal. Chem. 86 (2014) 11606.
[39] R. Ghaffarian, E. Pérez-Herrero, H. Oh, S.R. Raghavan, S. Muro, Adv. Funct. Mater. 26 (2016) 3382.
[40] D. Sun, R. Bai, W. Zhou, Z. Yao, Y. Liu, S. Tang, X. Ge, L. Luo, C. Luo, G.-f. Hu, Gut (2020).
[41] E.A. Franzosa, A. Sirota-Madi, J. Avila-Pacheco, N. Fornelos, H.J. Haiser, S. Reinker, T. Vatanen, A.B. Hall, H. Mallick, L.J. McIver, Nature Microbiology 4 (2019) 293.
[42] C. Staat, C. Coisne, S. Dabrowski, S.M. Stamatovic, A.V. Andjelkovic, H. Wolburg, B. Engelhardt, I.E. Blasig, Biomaterials 54 (2015) 9.
[43] J.P. Arab, M. Arrese, M. Trauner, Annu. Rev. Pathol. 13 (2018) 321.
[44] O. Beutel, R. Maraspini, K. Pombo-Garcia, C. Martin-Lemaitre, A. Honigmann, Cell 179 (2019) 923.
[45] D. Ramanan, R. Bowcutt, S.C. Lee, M. San Tang, Z.D. Kurtz, Y. Ding, K. Honda, W. C. Gause, M.J. Blaser, R.A. Bonneau, Science 352 (2016) 608.
[46] N. Segata, J. Izard, L. Waldron, D. Gevers, L. Miropolsky, W.S. Garrett, C. Huttenhower, Genome Biol. 12 (2011) 1.
[47] Y.L.W. Hang Yu Xu, Dun fang wang, xu ran, ma, hong Xiang Li, wei peng, yang, Acta Pharm. Sin. 52 (2017) 9.